Available online at www.sciencedirect.com
ScienceDirect
Advances in Space Research 42 (2008) 763–769
ADVANCES IN SPACE RESEARCH (a COSPAR publication)
www.elsevier.com/locate/asr

Dynamics of global electron content in 1998–2005 derived from global GPS data and IRI modeling

E.I. Astafyeva [a,*], E.L. Afraimovich [a], A.V. Oinats [a], Yu.V. Yasukevich [a], I.V. Zhivetiev [b]

[a] Institute of Solar-Terrestrial Physics SB RAS, 126, Lermontov Street, Irkutsk 664033, Russian Federation
[b] Institute of Cosmophysical Research and Radiowave Propagation, FEB RAS, 7, Mirnaya Street, Paratunka, Elizovskiy District, Kamchatka Region 684034, Russian Federation

Received 9 October 2006; received in revised form 2 November 2007; accepted 7 November 2007

Abstract

We analyzed the dynamics of global electron content (GEC) for the period 1998–2005 and compared the estimated GEC with variations of the 10.7-cm solar radio emission and with and with GEC values obtained with IRI-2001. We found a strong resemblance between the curves' shapes for the experimental and modeled GEC: strong semiannual variations are discernible in these series and both curves tend to increase the absolute GEC value during the period of maximum of solar activity. However, there are some significant distinctions, such as absence of 27-day fluctuations in the series of GEC computed by the IRI-2001. On the contrary, observational GEC reflects well dynamics of solar activity: 27-day variations of GEC are very similar to the ones of the index F10.7, but GEC undergoes a lagging of about of 30–60 h as compared to value of the F10.7 index. The relative amplitude of 27-day variations decreases from 8% at the rising and falling solar activity to 2% at the period of its maximum.

Keywords: GPS; Global electron content; Solar activity; IRI; F10.7

1. Introduction

It is known that conditions of the Earth's ionosphere are determined mainly by solar radiation within a wide range of wavelengths (Akasofu and Chapman, 1972; Hargreaves, 1979). Plenty of studies have been devoted to the investigation of variations of ionospheric parameters with solar activity (Balan et al., 1996; Jakowski et al., 1991, 2002; Kane et al., 1995; Liu et al., 2006; Ping et al., 2004; Stankov and Jakowski, 2006). Moreover, some attempts have been made to solve the inverse problem, i.e. to calculate solar flux characteristics from ionosphere observational data (Beynon and Brown, 1959; Nusinov, 2004). However, the main problem is in fact that observational tools provide information about the ionosphere changes around an area of observations, whereas globally there might be significant distinctions.

Recently, the global behavior of the major ionospheric parameters has been studied (Ping et al., 2004; Stankov and Jakowski, 2006). Besides, a new approach for studying of Sun–Earth connection was proposed for the first time by Afraimovich et al. (2006a,b). This approach lies in calculation of global electron content which is equal to the total number of electrons in the near space environment (from the ground up to 20,200 km). The method and the software of GEC estimation were developed at the Institute of Solar-Terrestrial Physics SB RAS. The main advantage of this approach is in the disappearance of local features of ionosphere and in determining of dynamics of global characteristics. Such new application of experimental data can be quite expedient for corrections of different ionosphere models that are widely used for ionosphere studying as well as for providing of effective satellite and ground-based radio system operating.

* Corresponding author. Tel.: +7 3952 564554; fax: +7 3952 511675.
E-mail address: elliada@iszf.irk.ru (E.I. Astafyeva).

0273-1177/$34.00
doi:10.1016/j.asr.2007.11.007

The objectives of this research are to analyze dynamics of global electron content during the 1998–2005 and to compare the observational GEC with IRI-2001 modeled GEC values and with solar activity parameters.

2. General information about the experiment: Calculation of GEC

2.1. Global ionosphere maps of total electron content

We have calculated GEC using global ionosphere maps (GIM) of vertical total electron content (TEC) generated on the basis of data from International GPS receivers network (Mannucci et al., 1998; Schaer et al., 1998). Nowadays, global TEC maps are calculated at several scientific centers: Geodetic Survey Division of Natural Resources Canada (EMRG) [http://www.nrcan-rncan.gc.ca/], Center for Orbit Determination in Europe, University of Berne, Switzerland (CODG) [http://www.cx.unibe.ch/], Jet Propulsion Laboratory of California Institute of Technology (JPLG) [http://www.jpl.nasa.gov/] and Grup Universitat Politecnica de Catalunya (UPCG) [http://www.upc.es/], European Space Agency Group (ESAG). In our paper we used data of JPLG and in the case of lack of JPLG data we used CODG data with the corresponding correction.

It should be noted that the scatter in the results from the various models used by the scientific groups, is on the order of 20–50% (http://www.vlba.nrao.edu/memos/sci/gps_ion/node3.html). The differences are the result of different assumed vertical profiles and perhaps different allotment of delay to instrumental effects and ionosphere. Besides, the receiver networks used are not always the same. However, despite different methods for the absolute vertical TEC reconstruction, the general idea is based on fitting of the optimal parameters of a selected model of the vertical electron density distribution (N(h)-profile). For such model values of the expected ionosphere correction to the distance to a satellite are calculated for real visual angles to satellite. Then calculated correction values are compared with measured ones and this process is repeated for different ionosphere models of N(h)-profile parameters till the minimal discrepancy is achieved. These minimal RMS values are presented in GIM output files. Then, for the "optimal" N(h)-profile the "vertical" TEC is calculated as averaged value of "vertical" TEC $I(t)$ for the corresponding elementary GIM cell.

The GIM are available from Internet site of the NASA's Crustal Dynamics Data Information System (ftp://cddisa.gsfc.nasa.gov/pub/gps/products/ionex/) in standard IONEX format; the files contain data of the vertical TEC for the entire globe. The size of the elementary GIM cell is 5° of longitude and 2.5° of latitude. For each moment of time the vertical TEC values $I_{i,j}$ can be obtained from 2-h time resolution IONEX files, where i and j indices are the numbers of a certain GIM cell.

2.2. Method of global electron content calculation

GEC is estimated using data of GIM by summation of the vertical TEC values $I_{i,j}$ multiplied by a cell's area $S_{i,j}$ over all GIM cells (Afraimovich et al., 2006a,b):

$$G(t) = \sum I_{i,j} \cdot S_{i,j} \tag{1}$$

We suggest a unit for GEC estimation is GECU that is equal to 10^{32} (Afraimovich et al., 2006a).

We calculated number of electrons for each GIM cell using formula (1) within a tube of a constant diameter, i.e. spherical divergence is not taken into account. The corresponding systematic error of GEC estimation depends on the form of the electron density profile and reaches ~10–15%. However, this factor influences mainly the absolute value of GEC, but not the form or character of GEC variations.

If estimations of TEC in each GIM cell are independent (as the first approximation, it can be accepted) then the relative error of GEC estimation is defined as

$$\eta = \frac{\sigma_{\mathrm{GEC}}}{m_{\mathrm{GEC}}} = \frac{\sqrt{\sum S_{i,j}^2 \sigma_{i,j}^2}}{\sum S_{i,j} I_{i,j}}, \tag{2}$$

where σ_{GEC}, $\mathrm{m}_{\mathrm{GEC}}$, $\sigma_{i,j}$ – GEC RMS, mean GEC, TEC RMS in GIM cell (i,j), respectively. If $S_{i,j} = S$, $\sigma_{ij}^2 = \sigma^2$, $I_{ij} = I$ then relative error will be equal to $\eta = \sigma/(I\sqrt{n})$, where $n = 5184$ – the number of GIM cells.

We have calculated the relative error of GEC estimations using (2) for several days of 2003 and 2004. According to our calculations, the relative error of GEC estimations does not exceed 0.3% and the error for GEC estimation is about 0.002–0.004 GECU. However, the values of TEC and TEC RMS in each GIM cell are not independent because in many cells there are no GPS sites and it is necessary to approximate the TEC values, then. So the error of GEC estimation is a little more significant. Nevertheless, it is less noticeable than that of the calculation of the vertical TEC for each GIM cell (about 10–20% – Mannucci et al., 1998; Schaer et al., 1998).

The high accuracy of GEC estimation allows us to carry out the detailed comparison between experimental and IRI modeled GEC series (see Section 3 and Table 1).

2.3. Modeling of GEC by the International Reference Ionosphere 2001 (IRI-2001)

Modeled GEC values were estimated using the well-known and widely used international empirical model International Reference Ionosphere (Bilitza, 2001; http://IRI.gsfc.nasa.gov). This model was recommended by the International Telecommunication Union ITU-R (ITU, 2004), as a suitable method for TEC estimations. The main parameter in the case of TEC calculation by the IRI-2001 is the upper height for electron density profile integration $h_{\max}$. It turned out that at the upper height $h_{\max} = 20{,}000$ km GEC values are overestimated for more

Table 1
Results of comparison between GEC-IRI and experimental GEC values

N	Year	Time window, days	$(G - M)/G$ (%)	RMS (%)
1	1998–2005	365	−1.5	5.0
2	1999	81	−1.4	4.3
3	2000	81	−1.3	7.0
4	2001	81	−1.6	10.7
5	2002	81	3.6	10.0
6	2003	81	−7.1	5.7
7	2004	81	−6.1	3.4
8	2005	81	−8.6	5.6
9	1999	10	−1.98	10.5
10	2000	10	−1.98	11.0
11	2001	10	−2.81	15.1
12	2002	10	2,88	13.7
13	2003	10	−7.8	11.0
14	2004	10	−6.5	8.6
15	2005	10	−9.3	9.2

than six times. This overestimation is related to the fact that the IRI electron density profile is close to the real ionosphere profile only up to the height 1500 km and it becomes almost constant above 1500 km (Coisson and Radicella, 2004, 2005). The value $h_{max} = 2000$ km results in the minimum absolute difference between the experimental and IRI modeled GEC dependencies. Therefore, all GEC estimations performed by the IRI-2001 were made for $h_{max} = 2000$ km (Afraimovich et al., 2006b).

In a new version of IRI the correction term of the topside density profile for the current IRI model will be included, as proposed by D. Bilitza (2004). Furthermore, NeQuick electron density topside will be included in the new IRI as an option for topside electron density calculations (Coisson et al., 2005). Apparently, it is very interesting to compare our results also with Parameterized Ionospheric Model (PIM; www.cpi.com) or the Global Core Plasma Model (GCPM; Gallagher et al., 1988), but this is a subject of future investigations.

GEC-IRI values $M(t)$ were calculated in two stages. First, IRI TEC values were calculated throughout the globe in latitude-longitude mesh points with step 5° along the longitude and 2.5° along the latitude during all time period with a step of 2 h. Then, the derived TEC values were integrated according to the formula (1).

2.4. Changes of solar activity

In general, solar activity level can be determined by several parameters characterizing solar irradiance and space weather near the Earth (for example, http://www.space-wx.com). Here we compared our experimental data with F10.7 solar activity index $F(t)$, which is equal to the solar radiation flux on the wavelength 10.7 cm in s.f.u. units (10^{-22} Wm^{-2} Hz^{-1}), and daily value of sunspot number Rsn(t).

We smoothed $G(t)$, $F(t)$ and $M(t)$ series with the time window of 10 days. Diurnal variations appear to be averaged and, therefore, significant effects of quick GEC changes cannot be distinguished (such as geomagnetic disturbances). These processes are the topics of a special study.

3. Experimental and modeled GEC changes from 1998 to 2005

In our investigation we have studied GEC alterations due to solar activity changes within a part of the 23rd solar cycle (1998–2005). For this period of time GEC value $G(t)$ varied from 0.8 to 3.2 GECU (Fig. 1a, black thick curve).

We calculated GEC-IRI values $M(t)$ using the IRI-2001 and we found a strong resemblance to the form of the experimental GEC curve for the period from 1998 to 2005 (Fig. 1b, black thick curve) but $M(t)$ has smaller absolute values of GEC (from 1 to 2.7 GECU). Besides, there are no 27-day variations in the series of $M(t)$, i.e. IRI-2001 does not take into account rotation of the Sun.

It can be noticed that $G(t)$ and $M(t)$ are characterized by significant semi-annual variations with maximum relative amplitude about 10% during the rising and falling parts of the solar activity period and up to 30% during the period of maximum (Fig. 1a and b). Maximums of dependencies are in equinoctial months.

We compared $G(t)$ series with solar activity index F10.7 that is equal to the 10.7-cm solar radio flux $F(t)$ (Fig. 1c) and we found good agreement between these variations. Resemblance between $G(t)$, $M(t)$ and $F(t)$ is more obvious for smoothed by one-year time window dependencies (Fig. 1d).

To make more detailed comparison between experimental $G(t)$ and IRI modeled $M(t)$ series we estimated the mean relative deviation $[G(t) - M(t)]/G(t)$ for all the years under consideration (Table 1). As one can see, the relative difference between $G(t)$ and $M(t)$ variations exceeds the difference between series during 1998–2005 smoothed by the one-year time window (line 1). The same conclusion is about seasonal variations $G(t)$ and $M(t)$ (lines 2–8). So the mean relative difference $[G(t) - M(t)]/G(t)$ increases to the end of 23rd cycle and reaches 9.3% (2005). However RMS $[G(t) - M(t)]/G(t)$ is maximum for the period of solar activity maximum: 15.1% (2001) and 13.7% (2002). Thus, the relative difference and RMS between GEC-IRI and experimental GEC series increase as smoothing time window decreases. Mainly this reflects the fact that IRI is a median model of the ionosphere and does not take into account day-to-day variations of the ionosphere parameters (e.g. 27-day variations).

4. Day and night values of GEC

For better understanding of physical mechanisms of the ionosphere dynamics it is of interest to estimate day G_d and night G_n values of GEC. To calculate G_d and G_n we carry out summation (1) only for those GIM cells that are located inside or outside the solar terminator border.

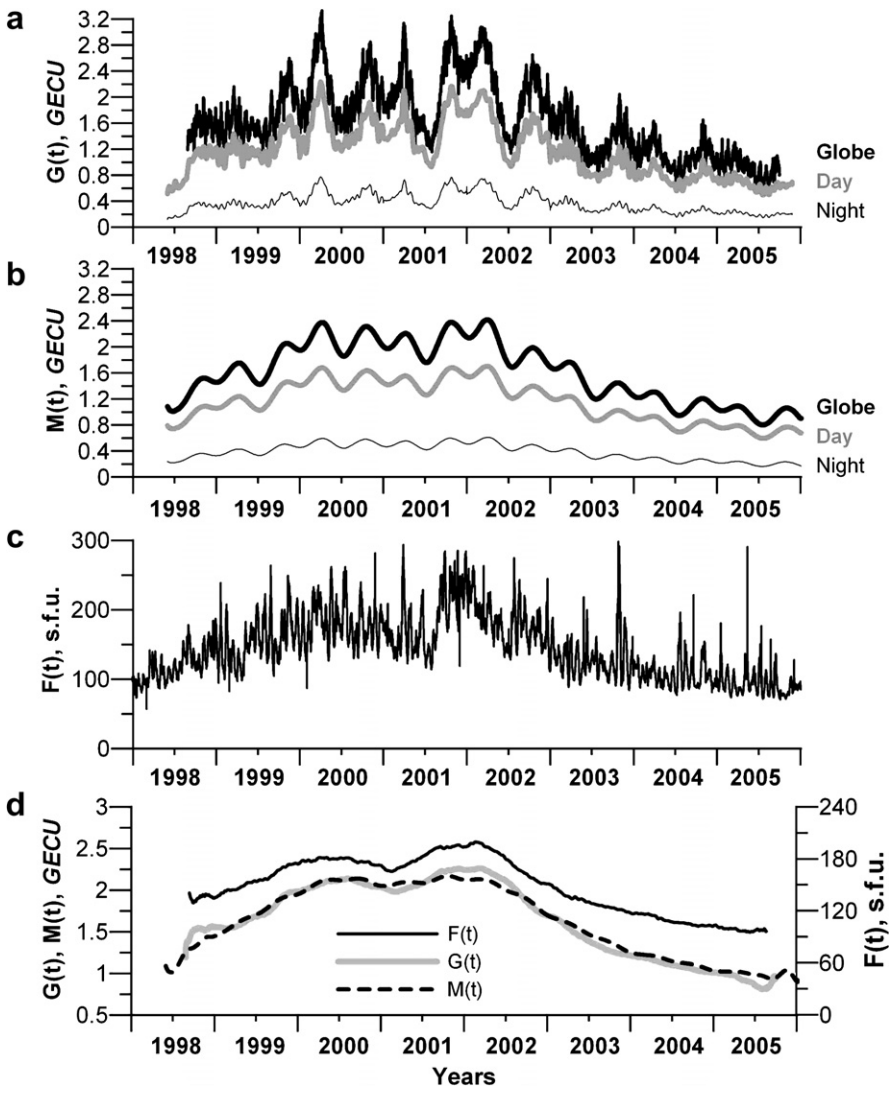

Fig. 1. (a) Experimental GEC variations $G(t)$ (black thick curve); (b) GEC, modeled by the IRI-2001 $M(t)$; (c) the 10.7-cm solar radio emission; (d) smoothed with the 365-day time window dependencies of $F(t)$, $M(t)$, $G(t)$. Gray thick and black thin curves show day and night values of $G(t)$ (a) and $M(t)$ (b).

Fig. 1a presents $G_d(t)$ and $G_n(t)$ values of the lighted and darken sides of the Earth (light gray and black thin curves). Fig. 1b shows the same dependencies for modeled by the IRI 2001 values $M_d(t)$ and $M_n(t)$. One can see that the experimental and modeled dependencies of GEC for the day and night sides of the Earth are very similar. Both day and night GEC dependencies have semiannual variations and differ from each other only by a constant value (by 0.5–2.0 GECU depending on the level of solar activity).

For more detailed comparison with IRI 2001 calculations we determined a ratio $R = G_d/G_n$ of GEC for the lighted and darken sides of the Earth, for both $G(t)$ and $M(t)$. Fig. 2 illustrates difference between experimental and model values of $R(t)$ within the time scale of 1 year for the 1999 (a), 2001 (b) and 2003 (c).

It turned out that $R(t)$ ratios are effected by seasonal variations: the maximum of R ratio values were observed during the periods of solstice (in winter and summer) and minimum in the equinoxes. We have obtained such seasonal dependence for both experimental $G(t)$ and IRI $M(t)$ data.

The observed effect may be caused by the fact that the ionosphere has a number of anomalies and asymmetries which have not been well investigated yet. Rishbeth and Muller-Wodarg (2006) and Mendillo et al. (2005) described in detail the global asymmetry of the ionospheric F2-layer showing "more ionosphere" in January than in July. Rishbeth and Muller-Wodarg (2006) emphasized that the F2-layer annual asymmetry between January and July is typically 30% while the asymmetry of ion production due to the annual variation of the Sun-Earth distance is only around 7%. Therefore, the observed seasonal dependence due to inclination of the axis of the equator, affects the ratio of dayside and nightside ionization values.

It is obvious that the values of $R(t)$ for modeled GEC are greater than for the experimental one, i.e. IRI produces

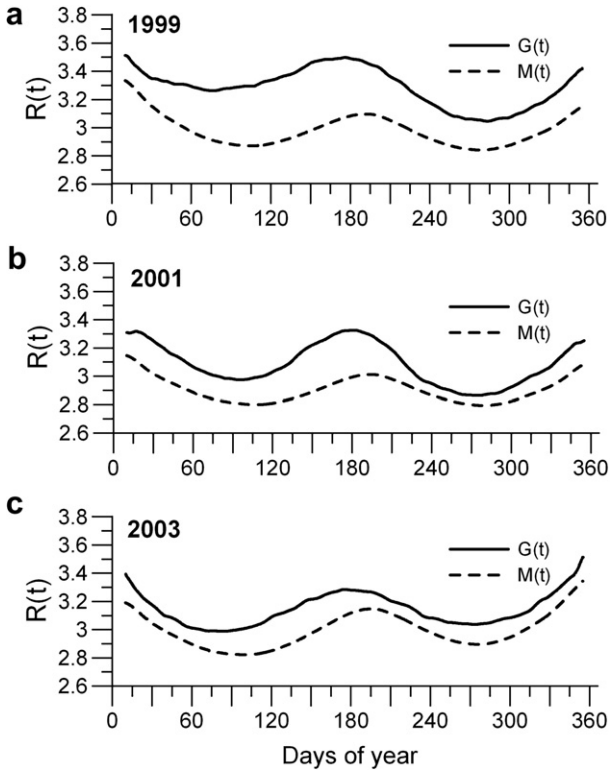

Fig. 2. Ratio $R(t)$ of the day and night values for GEC (black curves) and for modeled GEC (dotted curves) for the 1999, 2001, 2003.

significantly overestimated nighttime GEC. Besides, dependencies $R(t)$ for $G(t)$ and $M(t)$ are not phased, i.e. peaks in $R(t)$ for experimental GEC differ in time from peaks for $M(t)$ and there is also time difference for the minimal values of $R(t)$ (Fig. 2).

5. 27-day variations of GEC. Comparison with F10.7 variations

As it was mentioned above, GEC has 27-day variations related to the Sun rotation. Fig. 3 shows time dependencies of relative amplitude of 27-day variations for $G(t)$ and $F(t)$. GEC variations were calculated for each day within the interval from 17.00 to 21.00 UT. Then these data series were filtered within the period range from 20 to 40 days and normalized on background values of the $G(t)$ and $F(t)$, respectively. Relative amplitudes of 27-day variations of $G(t)$ and $F(t)$ are shown on Fig. 3a: $dG/G(t)$ – thick curve; $dF/F(t)$ - thin curve. Fig. 3b presents $G(t)$ variations (thick curve) and F10.7 variations (thin curve), smoothed with the 10-day time window (for the year 2003). Correlation analysis for all data from 1998 to 2005 shows high resemblance between 27-day variations of the $G(t)$ and $F(t)$ (maximum correlation coefficient is more than 0.8).

We found that 27-day GEC variations lag for 1.5–2.5 days after the corresponding F10.7 variations (Fig. 3a). It is known that response of the ionosphere to changes of the ultraviolet radiation flux is determined by the lag time

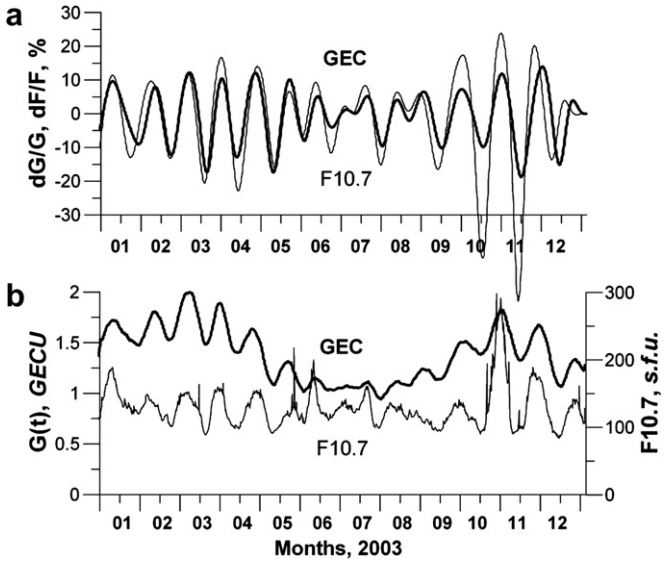

Fig. 3. (a) Relative amplitude of 27-day variations of $G(t)$ and $F(t)$, filtered in the time period range 20–40 days; (b) $G(t)$ and $F(t)$ variations, smoothed with the 10-days time window.

and the recombination time constants, which is about 1 h (Bryunelli and Namgaladze, 1988; Namgaladze et al., 1991). The founded lag of the 27-day GEC variations relative to corresponding alterations of the F10.7 flux can be caused by significantly greater time constants that characterize processes in the thermosphere as GEC variations are caused not only by changes of the solar ionizing radiation but the processes in the thermosphere as well. As solar radiation flux increases, ionizing the ionosphere and heating the thermosphere, both the temperature and the total density of the atmosphere increase, and the speed and direction of the neutral wind change (Bryunelli and Namgaladze, 1988). It is also necessary to take into account that time scales of the electron content variations in the Earth's plasmasphere change within the time range from 2 to 5 days (Hargreaves, 1979). However, the detailed analysis of the mechanisms responsible for the found lag of the 27-day GEC variations relative to the corresponding changes of the F10.7 flux is a more difficult problem, its solution expects the use of physical models of the ionosphere, for example (Namgaladze et al., 1991).

Fig. 4 presents the envelope of 27-day variations of GEC (G27(t), thick curves) and of 10.7-cm solar radiation flux (F27(t), thin curves) during the period 1998–2005, smoothed by 365-day time window (a) and 81-day window (b). To estimate the envelope of 27-day variations amplitude we squared the dependence $dG/G(t)$ and, then, we smoothed the envelope of $[dG(t)/G(t)]^2$. One can see from Fig. 4 that maximal deviation of the relative amplitude G27(t) decreases from 8% at the rising and falling solar activity to 2% at the period of its maximum. But 27-day variations amplitude of the F10.7 can reach 14% (Fig. 4a, thin curve). Thus, such dependence shows dynamics of powerful active formations on the Sun surface (Mordvinov and Plyusnina, 2001; Mordvinov and Willson, 2003).

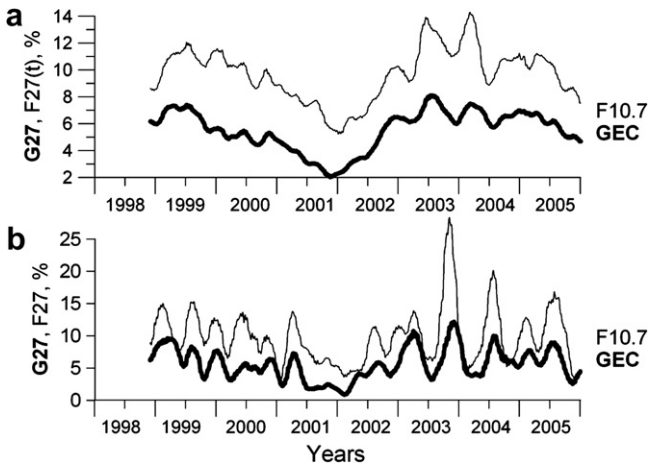

Fig. 4. The envelope of 27-day variations G27(t) of GEC and F27(t) of the 10.7-cm solar radio emission smoothed with time window of 365 days (a) and of 81 days (b).

6. Conclusion

Global electron content is a new ionosphere parameter that reflects changes of solar activity; its absolute value varied from 0.8 GECU at the minimum of solar activity to 3.2 GECU at the maximum (in the 1998–2005). GEC data series $G(t)$ contain 27-day variations that are very similar to the ones of the index F10.7 $F(t)$; however, $G(t)$ lags in time for 1.5–2.5 days from $F(t)$.

IRI-2001 sufficiently well and adequately reflects changes of the global ionosphere, showing semi-annual and 11-year variations. However, the modeled data $M(t)$ have some significant distinctions from the observational ones, such as overestimation of $M(t)$ values for the night side of the Earth and absence of 27-day variations in $M(t)$ series.

The data presented in our paper are of considerable interest for the reconstruction of solar radiation characteristics from the ionosphere observational data and for studying of the ionization processes caused by solar ultraviolet radiation. Besides, our results are important for calibration and correction of ionosphere models.

Acknowledgements

We are grateful to academician G.A. Zherebtsov, Drs. V.V. Pipin, V.G. Eselevich, A.V. Mordvinov, L.A. Plyusnina for their support and interest in our work and E.A. Kosogorov for his help in programming. We acknowledge the Jet Propulsion Laboratory of California Institute of Technology (JPLG) and NASA's Crustal Dynamics Data Information System for GIM and the Dominion Radio Astrophysical Observatory (DRAO, Canada) for the data of 10.7-cm radio emission.

We thank the two reviewers whose useful suggestions improved the quality of the paper.

The work was done under support of the Russian Foundation for Basic Research (RFBR Grant No. 07-05-00127 and RFBR-GFEN Grant N 06-05-39026).

References

Akasofu, S.I., Chapman, S. Solar-Terrestrial Physics. Pergamon, Oxford, 512 pp., 1972.

Afraimovich, E.L., Astafyeva, E.I., Zhivetiev, I.V. Solar activity and global electron content. Doklady Earth Sciences 409A (N6), 921–924, 2006a.

Afraimovich, E.L., Astafyeva, E.I., Oinats, A.V., Yasukevich, Yu.V., Zhivetiev, I.V. Global electron content as a new index of solar activity. Comparison with IRI modeling results IRI news 13 (N1), A5, October 2006, 2006b.

Balan, N., Bailey, G.J., Su, Y.Z. Variations of the ionosphere and related solar fluxes during solar cycles 21 and 22. Adv. Space Res. 18 (3), 11–14, 1996.

Beynon, W.J.G., Brown, G.M. Region E and solar activity. J. Atm. Terr. Phys. 15, 168–174, 1959.

Bilitza, D. International reference ionosphere. Radio Sci. 36 (2), 261–275, 2001.

Bilitza, D. A correction for the IRI topside electron density model based on Alouette/ISIS topside sounder data. Adv. Space Res. 33 (6), 838–843, 2004.

Bryunelli, B.E., Namgaladze, A.A. Physics of the Ionosphere. Nauka, Moscow, 528 pp. (in Russian), 1988.

Coisson, P., Radicella, S.M. The IRI topside parameters. Adv. Radio Sci. 2, 249–251, 2004.

Coisson, P., Radicella, S.M. Ionospheric topside models compared with experimental electron density profiles. Ann. Geophys. 48 (3), 497–503, 2005.

Gallagher, D.L., Craven, P.D., Comfort, R.H. An empirical model of the earth's plasmasphere. Adv. Space Res. 8, 15–24, 1988.

Hargreaves, J.K. The Upper Atmosphere and Solar-Terrestrial Relations. Van Nostrand Reinhold Co Ltd., New York, 298 pp., 1979.

ITU. Ionospheric propagation data and prediction methods required for the design of satellite services and systems, Recommendation ITU-R P.531–7, 2004.

Jakowski, N., Fichtelmann, B., Jungstand, A. Solar activity control of Ionospheric and thermospheric processes. J. Atm. Terr. Phys. 53, 1125–1130, 1991.

Jakowski, N., Heise, S., Wehrenpfennig, A., Schluter, S., Reimer, B. GPS/GLONASS-based TEC measurements as a contributor for space weather forecast. J. Atm. Terr. Phys. 64 (5–6), 729–735, 2002.

Kane, R.P., de Paula, E.R., Triverdi, N.B. Variations of solar EUV, UV and ionospheric f_0F2 related to the solar rotation period. Annales Geophysicae 13, 717–723, 1995.

Liu, L., Wan, W., Ning, B., Pirog, I.M., Kurkin, V.I. Solar activity variations of the ionospheric peak electron density. J. Geophys. Res. Ill, A08304, doi:10.1029/2006JA011598, 2006.

Mannucci, A.J., Wilson, B.D., Yuan, D.N., Ho, C.M., Lindqwister, U.J., Runge, T.F. A global mapping technique for GPS-derived ionospheric TEC measurements. Radio Sci. 33 (3), 565–582, 1998.

Mendillo, M., Huang, C.-L., Pi, X.-Q., Rishbeth, H., Meier, R.R. The global asymmetry in ionospheric total content. J. Atmos. Solar Terr. Phys. 67, 1377–1387, 2005.

Mordvinov, A.V., Plyusnina, L.A. Coherent structures in the dynamics of the large-scale solar magnetic field. Astronomy Reports 45, 652–658, 2001.

Mordvinov, A.V., Willson, R.C. Effect of large-scale magnetic fields on total solar irradiance. Solar Phys. 215, 5–16, 2003.

Namgaladze, A.A., Korenkov, Yu.N., Klimenko, V.V., Karpov, I.V., Surotkin, V.A., Naumova, N.M. Numerical modelling of the thermosphere–ionosphere–protonosphere system. J. Atm. Terr. Phys. 53 (11/12), 1113–1124, 1991.

Nusinov, A.A. The Ionosphere as a natural detector for studying long-period variations in the fluxes of solar geoeffective radiation. Geomagnet. Aeronomy 44 (6), 718–725, 2004.

Ping, J., Matsumoto, K., Heki, K., Saito, A., Callahan, P., Potts, L., Shum, C.K. Validation of Jason-1 Nadir Ionosphere TEC Using GEONET. Marine Geodesy 27 (3–4), 741–752, 2004.

Rishbeth, H., Muller-Wodarg, I.C.F. Why is there more ionosphere in January than in July? The annual asymmetry in the f2-layer. Annales Geophysicae 24, 3293–3311, 2006.

Schaer, S., Beutler, G., Rothacher, M. Mapping and predicting the ionosphere. In: Proceedings of the IGS AC Workshop, Darmstadt, Germany, 1998.

Stankov, S., Jakowski, N. Topside ionospheric scale height analysis and modelling based on radio occultation measurements. J. Atm. Sol. Terr. Phys. 68 (2), 134–162, 2006.